REPORT DOCUMENTATION PAGE

Form Approved
OMB No. 0704-0188

1. AGENCY USE ONLY (Leave blank)	2. REPORT DATE	3. REPORT TYPE AND DATES COVERED
	29 Mar 95	Final 30 Sep 95 - 29 Mar 95

4. TITLE AND SUBTITLE
E-Beam Addressed Spatial Light Modulator Employing Electron Trapping Materials

5. FUNDING NUMBERS
N00014-94-C-0242

6. AUTHOR(S)
Xiaojing Lu, Xiangyang Yang, Charles Y. Wrigley, Richard Bradley and Janos Meszaros

7. PERFORMING ORGANIZATION NAME(S) AND ADDRESS(ES)
Quantex Corporation
2 Research Court
Rockville, MD 20850

8. PERFORMING ORGANIZATION REPORT NUMBER
N/A

9. SPONSORING/MONITORING AGENCY NAME(S) AND ADDRESS(ES)
Office of Naval Research
ONR 313, Ballston Tower One
800 North Quincy Street
Arlington, VA 22217-5660

10. SPONSORING/MONITORING AGENCY REPORT NUMBER

11. SUPPLEMENTARY NOTES

12a. DISTRIBUTION/AVAILABILITY STATEMENT

12b. DISTRIBUTION CODE

13. ABSTRACT (Maximum 200 words)

Spatial light modulators (SLMs) play a critically important role in optical signal processing and optical computing. A novel electron beam addressed emissive SLM which combines high performance polycrystalline electron trapping (ET) materials with an advanced field-emitter array is being developed. The proposed SLM combines high resolution (> 100 lp/mm), high SBP (≥ 1000x1000), high frame rate (≥ 1 KHz), high contrast ratio (> 10^3:1) and low drive voltage (< 15 V) in a single device. The additional features of the proposed SLM are its wide variety of operation modes and electrical and optical dual-addressability. Such a SLM, if successfully developed, will surely have substantial impact on optical processing technology. During the Phase I efforts, a review of field emitter arrays has been done to show that it has the merits of electrical-addressability, high space-bandwidth product (SBP), low drive voltage compatible with IC driving circuitry, and high update speed. The device architecture has been investigated and the design of two prototype devices has been provided. The performance of polycrystalline ET thin films with both Al_2O_3 and Al anode electrode layers under e-beam and IR excitation has been evaluated to show that the bias voltage can be less than 5-6 KeV. These results not only have determined the feasibility of the proposed SLM, but also provided a solid foundation for the development of a working prototype to be fabricated in Phase II.

14. SUBJECT TERMS	15. NUMBER OF PAGES
Spatial light modulator, electron trapping materials, field emitter array, optical processing technology, optical signal processing, optical neurocomputing	27
	16. PRICE CODE

17. SECURITY CLASSIFICATION OF REPORT	18. SECURITY CLASSIFICATION OF THIS PAGE	19. SECURITY CLASSIFICATION OF ABSTRACT	20. LIMITATION OF ABSTRACT
unclassified	unclassified	unclassified	UL

E-BEAM ADDRESSED SPATIAL LIGHT MODULATOR EMPLOYING ELECTRON TRAPPING MATERIALS - PHASE I

Contract No.: N00014-94-C-0242

Final Report

March 29, 1995

Submitted by:

Xiaojing Lu
Xiangyang Yang
Charles Y. Wrigley
Richard Bradley
Janos Meszaros

Quantex Corporation
2 Research Court
Rockville, Maryland 20850

Research supported by Ballistic Missile Defense/Innovative Science and Technology and managed by the Office of Naval Research.

TABLE OF CONTENTS

LIST OF FIGURES

1. INTRODUCTION

The goal of the research program reported herein is to develop a novel electron beam addressed emissive spatial light modulator (SLM) which combines an advanced field-emitter array with high performance polycrystalline electron trapping (ET) materials. The objective of the Phase I effort was to determine the feasibility of fabricating the e-beam addressed SLM. It has been funded by the BMDO via the Office of Naval research. The Phase I work was implemented from September 30, 1994 to March 29, 1995.

1.1 Background of the project

There has been considerable research effort over the last three decades in the area of optical signal processing and computing. The great interest was primarily stimulated by many potential advantages of optical processing such as high SBP and time-bandwidth products. They are inherently two-dimensional (2-D) and parallel that optical signals propagate through 3-D space in parallel channels without interference and cross talk.. All these advantages, however, are still potential in most optical processing systems, in which any progress is severely hampered by the absence of high performance SLMs -- key components and fundamental building blocks of optical processing architectures. The state-of-the-art SLMs include magnetooptic SLMs [1], acoustooptic devices [2], liquid crystal SLMs [3-5], deformable mirror arrays [6], microchannel SLMs [7] self-electro-optic effect (SEED) devices [8], etc. [9,10]. The mechanism and performance levels of these currently available SLMs vary over a broad range. Some SLMs are featured by fast refresh speed and others possess large SBP. The trade-offs among different specifications (e.g., between resolution and speed) of the SLMs are very common so that they have rather limited overall performance. It is a widely accepted fact that the low performance of SLMs has become a major technological hurdle for optical signal processing and optical computing [9]. In order to fully take advantage of photonics over electronics, high performance SLMs, particularly based on new and innovative technologies and materials, must be developed.

ET materials are new optical materials developed by Quantex Corporation [11]. They are wide band-gap II-VI semiconductor compounds with two specific rare earth dopants. During the last several years, ET materials, particularly ET thin films, have been applied in several optical processing architectures as a spatial light rebrodcaster (SLR) or an optically driven optically addressed SLM [12-16]. The observed properties of these ET material based devices are very promising. The response time of ET materials is on the order of ten nanoseconds [12]. The linear dynamic range of the photoluminescent emission covers 4 orders of magnitude, which can lead to an extremely high contrast ratio and large modulation index [12]. In optical neurocomputing, this translates into wide dynamic range connectivity matrixes which are badly needed in the implementation of learning algorithms. The ET thin films currently possess a resolution of over 100 lp/mm [17] and have the potential to reach 1,000 lp/mm if fabricated in monocrystalline forms. The SLMs based on ET materials have the capability of incoherent-to-coherent conversion. Nevertheless, the wide spread of ET based SLRs and SLMs has been limited by the lack of electrical-addressability, which prevents their direct interfacing to a computer or other electronic units.

This drawback can be readily overcome by combining the ET based device with a field-emitter array of SRI International [18-20]. The field-emitter array comprises a large amount of very small field emission tips that are positioned close to an accelerating electrode (or gate). A single emitter occupies an area of about 1 μm^2, and as many as 10^7 emitter tips can be packed into a 1 cm^2 array. SRI's present capabilities allow up to 10^{10} identical emitters to be fabricated on a 5-in diameter silicon wafer. This is compatible with ET thin film and can lead to a SLM with high resolution and large SBP. The emitters can be matrix-addressed by an electrical signal [19]. This offers the proposed SLM electrical addressability. Scientists at Westinghouse Research Lab have reported the possibility of addressing the field-emitters by visible light [21]. This will lead to optical-addressability of the proposed SLM, and therefore provide the device a unique feature of optical and electrical dual-addressability. The proposed SLM therefore offers more versatility and application flexibility than all the state-of-the-art SLMs. It also provides the system developer a more powerful device for use in developing innovative optical processing and neurocomputing architectures that are not implementable with currently available SLMs, either optically addressable or electrically addressable.

Furthermore, when the ET material is excited by electron beam, the electron trapping efficiency has been proven to be substantially higher than that exhibited for visible (blue) light. The integration with field-emitter array will not only furnish the ET based SLM electrical-addressability, but also increase its quantum efficiency which will lead to high frame speed and high modulation index.

In order to fabricate an electrical addressed SLM with ET materials and field emitter array, we investigate their performances and develop the device archtecture. The proposed e-beam addressed SLM, if successfully developed, will surely have substantial impact in optical processing and computing technologies. The manufacturing cost is expected to be lower than many of the currently available SLMs. The commercial breakthrough can be envisioned when the cost-effective device with 1000x1000 pixels and 1 KHz frame rate becomes available.

1.2 PHASE I RESEARCH OBJECTIVES

The primary goal of the Phase I efforts was to develop a novel e-beam addressed emissive SLM that combines the advanced field-emitter array and high performance polycrystalline ET thin films. In order to achieve this goal, the following objectives were pursued, as stated in the Phase I proposal.

1. To review the field-emitter technology and study its compatibility with ET thin films.

2. To evaluate the performance of ET thin film with two thin layers of aluminum and oxide under both e-beam and IR fluences.

3. To investigate the device architecture so that the ET thin film and field emitter array can be integrated into a rugged device.

4. To conduct preliminary design of a cost-effective electron-beam addressed SLM with high performance.

5. To perform an investigation of various applications of the proposed device.

2. RESEARCH PERFORMED AND RESULTS OBTAINED

The Phase I effort was divided into five tasks, consisting of (1) review of field-emitter array technology, (2) evaluation of polycrystalline ET thin film for e-beam addressability, (3) investigation of the device architecture, (4) engineering design of a prototype device, (5) investigation of various applications of the proposed device. The work performed on these tasks and results obtained are reported as follows.

2.1 Task 1 - Recent Progress in Field-Emitter Array Technology

The key feature of the proposed SLM is the integration of Quantex's ET thin film and SRI International's field-emitter array. We have reviewed the field-emitter technology and its compatibility with ET thin films as well as its recent progress.

The SRI field-emitter array is an attractive microelectronic device that can be fabricated on any flat, smooth, vacuum-compatible substrate [18-20]. The substrate can be conducting or insulating, depending upon the application. The basic configuration of a matrix-addressable field-emitter array is shown in Fig.1. Molybdenum film strips are deposited on a silicon substrate as base electrodes. The substrate (with base electrodes) is covered with an insulating layer of thermally grown silicon dioxide (SiO_2). The SiO_2 is then coated with another layer of molybdenum film strips with their direction orthogonal to that of the base electrode strips. An array of holes about 1 μm in diameter is patterned using a multiple-electron-beam-lithography system. Next, the holes are etched through the SiO_2 to the base electrode, using the molybdenum as an etch mask. Finally, molybdenum cones are formed in the cavity by a thin-film deposition process with their bases on the base electrode strips and their tips in the plane of the top molybdenum film, as shown in Fig.1. The process could be performed with a variety of metals and insulators. Since the emitters do not utilize the semiconductor properties of single crystal silicon, glass or other inexpensive vacuum-compatible materials could be used for the substrate.

When a voltage is applied between the gate film and base electrode, electrons are emitted from the metal tips. A single tip can produce a current exceeding 10 μA. To generate a 2-D electron emission distribution, the emitter tips are addressed in one direction by strips of base film and in the orthogonal direction by the gate film strips. It should be noted that each pixel could comprise a number of emitter tips (e.g., 4x4, etc.) in order to deliver ample current to the target (e.g., ET film). Scientists at SRI have demonstrated the capability to fabricate up to 10^{10} identical emitters on a 5-in diameter silicon wafer. If each pixel contains 5x5 emitter tips, a SLM with 2000x2000 pixels can be developed with such a field-emitter array.

Current density and transconductance (slope of anode current versus gate voltage curve)

are important cathode parameters for many applications. The current density is directly related to the packing density of the tips in the emitter array, and the transconductance is proportional to the total number of tips in the array. At present, the smallest hole that can be achieved with the multiple-electron-beam-system used is about 0.5 μm in diameter so that the packing density is increased to 6.4 X 10^7. Recent efforts have been directed toward investigating means for increasing the transconductance of Spindt-type cathodes.

The factors that affect the transconductance ($\partial I / \partial V$) of a Spindt cathode are the effective work-function of the emitter tip ϕ, the emitter-tip field-enhancement factor β and the total emitting area ($n\alpha$) where n is the number of tips, and α is the average emitting area per tip. The value ϕ is a property of the emitter-tip material, crystallography and the condition of the emitter surface. The factor β is a geometric parameter and is dependent mostly on the emitter-tip radius, gate-aperture diameter and the position of the emitter tip relative to the plane of the gate electrode. These parameters are related through the Fowler/Nordheim equation:

$$I = \frac{n\alpha A(\beta V)^2}{\phi} e^{\frac{-B\phi^{3/2}}{\beta V}} \qquad (1)$$

If asuume that $a = \frac{n\alpha A\beta^2}{\phi}$ and $b = \frac{B\phi^{3/2}}{\beta}$, then the transconductance at a given operating point can be determined by:

$$\frac{\partial I}{\partial V} = \frac{I}{V}(2 + \frac{b}{V}) \qquad (2)$$

At first glance, this relationship would seem to suggest that a maximum transconductance can be obtained by minimizing β and maximizing ϕ. This is only true when working at very high emission levels. SRI has found that when it is necessary to work at very high emitter-tip loading (i.e. in the 100 μA/tip range); increasing the effective emission area produces the most rewarding results with regard to transconductance. On the other hand, increasing β by sharpening the emitter tip to lower the operating voltage is effective at low to moderate emission levels, however this approach can actually reduce the transconductance at high performance (high tip loading) levels due to a reduction in the average emission area per tip (α).

SRI has investigated methods for fabricating Spindt cathode array with smaller emitter, gate aperture dimensions, and increased packing densities; along with studies of processing techniques for improving cathode performance. The results have been rewarding with reductions in driving voltage requirements by factors of about 3 for a given emission level having been achieved. The most fruitful approach has been to reduce the diameter of the gate aperture to sub-micron dimensions by utilizing recent advances in lithography technology in combination with advances in emitter-cone formation techniques. In addition, surface studies have shown that hydrogen-plasma cleaning of the emitter tips prior to applying voltage can increase stability and lower the operating voltage significantly, apparently by removing high work-function contaminates from the emitter surface[22].

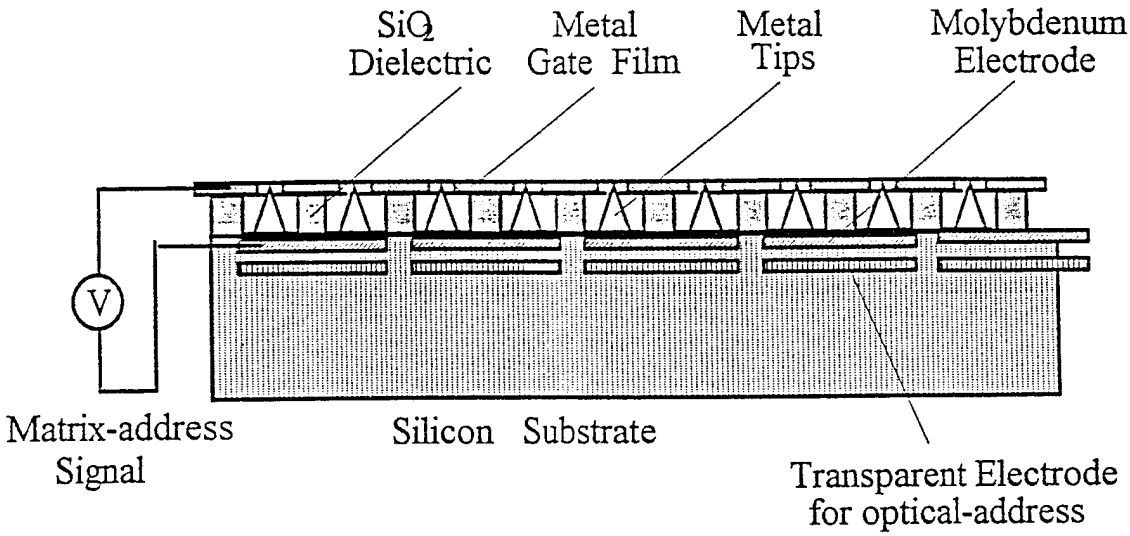

Fig.1 Field emitter array with matrix-addressing capability

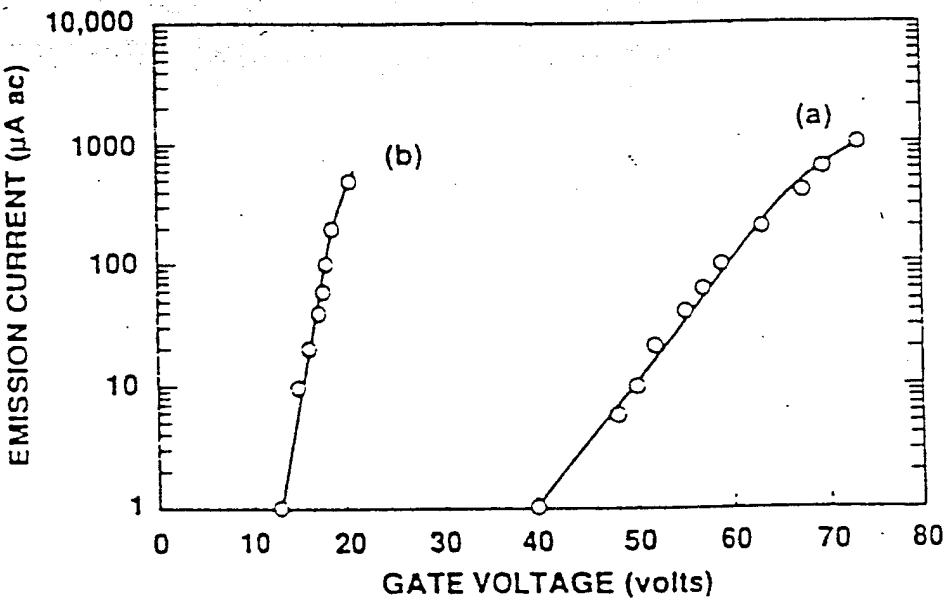

Fig.2 Current-voltage characteristics of a 10,000-emitter array (a) prior to cesiation, (b) optimum cesiation [20].

It has been shown experimentally that reducing the dimensions of the emitter in the array and increasing the emitter-tip packing density can result in significant reductions in operating voltage. An average emission of 15 μA/tip was produced from a 1000-tip array with an applied voltage of about 70 V[23], and 66 V produced 20 μA/tip from a sub-micron dimensioned (0.4 μm gate-aperture diameter) 100-tip array[24]. In very recent results, an emission current density of 2000 A/cm^2 averaged over the area occupied by a 100-tip array was demonstrated. Subsequent scanning-electron microscope examination of this emitter array showed no detectable damage to the cathode. In addition, in an ongoing test a Spindt cathode has been used to excite a phosphor (ZnO:Zn) continuously far over 2 years with a stability that is quite acceptable for display purposes. During this time there has been no trend toward degradation of the emission from the cathode. Tests with other phosphors that had not been carefully processed demonstrated that this long-term stability requires a careful selection of materials and rigrous processing to minimize contaminants in the system.

Finally, it has been shown that the voltage required to produce a given emission level from a cathode array can be reduced by about a factor of 3 by in-situ deposition of thin layers of stable electropositive materials (e.g. TI, Zr, and Hf) onto the emitter surface[25]

Regarding the transconductance (the current-voltage chracteristics), another promising candidate is the Cesiated thin film array [20] which requires only a control voltage less than 10 V, as shown in Fig.2, and is convenient for addressing by integrated circuit (IC) drivers, which would enable direct programmability by computer controllers.

2.2 Task 2 - Evaluation of Polycrystalline ET Thin Film

The Quantex ET materials are optically stimulable phosphors composed of IIa-VIb compounds (e.g., SrS, CaS, or mixtures of the two) doped with two rare earth dopants, such as Eu^{2+}/Sm^{3+}, or Ce^{3+}/Sm^{3+} [11]. These materials are wide-bandgap semiconductors (4.3 to 4.4 eV), and the dopants introduce new energy levels within the bandgap of the IIa-VIb materials. As a result, it is possible to induce electron transitions within and between the dopants by appropriate stimulation. For example, by exciting a Eu^{2+}/Sm^{3+} doped ET material with approximately 490 nm wavelength photons, it is possible to excite an electron from the ground state of Eu^{2+} to an excited state from which it can tunnel to and become *trapped* at a neighboring Sm^{3+} site. Once trapped, the electron can be photostimulated by approximately 1 μm wavelength infrared photons, releasing it back to the Eu site; relaxation of the electron back to the Eu^{2+} ground state then results in the emission of characteristic wavelength photons. With these processes, it is then possible to "write" to the material with 490 nm photons and "read" the information back with 1 μm (near IR) photon stimulation.

In the case of the Ce^{3+}/Sm^{3+} dopant combination, the same trapping and photostimulation process also occurs with the key difference that the "write" process is achieved with ionizing radiation (i.e., electrons, X-rays, etc.). Specifically, when the material is exposed to an e-beam, bound electron-hole pairs (excitons) are generated within the host crystal. These excitons rapidly lose energy and recombine at Ce^{3+} sites, and as a result, transfer energy to Ce^{3+}

ground-state electrons. The ground-state electrons are then excited to a higher energy level from which they tunnel to a neighboring Sm^{3+} where they become trapped, as with the Eu^{2+}/Sm^{3+} dopant combination. The read process is achieved as before by stimulation with 1 μm IR wavelength photons.

The dynamics of ET films under simultaneous e-beam writing and IR readout was established. When an ET film is written to by an e-beam, if the effect of fluorescence is negligible, the analytic model can be developed as

$$\frac{dn(t)}{dt} = \alpha I_{e(t)} - \beta n(t) I_{IR}(t) \tag{3}$$

$$I_o(t) = \gamma n(t) I_{IR}(t) \tag{4}$$

where n(t) is the trapped electron density; $I_e(t)$, $I_{IR}(t)$, $I_o(t)$ represent the intensities of writing e-beam, stimulating IR light and emitted orange light, respectively; α, β, and γ are dimensional constants for for e-beam, IR and orange light. If the IR illumination is constant, the e-beam intensity driven by the X-Y matrix circuit is expressed by

$$I_e(t) = A \sum \delta(t - kT) \tag{5}$$

where T is the frame time. The impulse A is $A \approx I_E t_0$ where I_E is the e-beam intensity and t_0 is the time during which each row of pixels is being addressed by the driver circuit. Eq. 1 is easily solved so that the electron trap density n(t) is for kT < t < (k+1)T (k >>1)

$$n(t) = A\alpha \frac{\exp(-\beta I_{IR}(t - kT))}{(1 - \exp(-\beta I_{IR} T))} \tag{6}$$

The parameter β has been measured [26], $\beta \approx 0.02 m^2/J$ for IR wavelength 880 nm. For a typical frame time T = 10 ms and IR intensity $I_{IR}(t)$ = 1 mW/cm^2, the factor $\beta I_{IR} T (\approx 2x10^{-3})$ is much less than one. Thus a simplied equation is obtained as

$$n(t) = \frac{\alpha}{\beta I_{IR}} \frac{I_E t_0}{T} \tag{7}$$

The above equation shows that since the slow charging and discharging dynamics of ETs, the electron trap density is effectively at a steady state equilibrium under this typical operating condition, as it is being equivalently addressed by a constant e-beam intensity $I_E t_0 / T$.

ETs are basically wide bandgap alkaline earth sulfides doped with two types of selected rare earth elements[11]. A typical example is $SrS:Eu^{2+},Sm^{3+}$. Figure 3 shows the enegy band diagram of $SrS:Eu^{2+},Sm^{3+}$ .The II-VI compond host SrS has a wide bandgap of ~ 4.3 eV. The electron trapping mechanism is due to the different electronic properties of Eu^{2+} and Sm^{3+}, namely, Eu^{2+} has ability to trap holes to become Eu^{3+}, and Sm^{3+} has ability to trap electrons to become Sm^{2+}. When ETs are written by electron beam, the energetic electrons strike and penetrate into the ET film so that the high energy electrons lose their enery through collisions with the host lattice and create large numbers of electron-hole pairs in the conduction and valence

bands of the host, respectively. The following processes are possible[27]:

1. Process σ1 - An electron is trapped in a Sm^{3+} site ⇒ a Sm^{2+} ground state (level 3)
and a hole is trapped in a Eu^{2+} site leaving behind Eu^{3+}

2. process σ2 - An electron is trapped in Sm^{3+} ⇒ Sm^{2+} ground state .
A hole is trapped ⇒ Sm^{3+} in excited state (level 6)
Relaxation from level 6 ⇒ ground state (5) produce fluorescence emission

3. process σ3a - The electrons tunnel to Sm^{3+} & fall to level 3 ⇒ Eu^{3+}ions & Sm^{2+}ions

σ3b - Electrons fall from level 2 to level 1 ⇒ fluorescent orange light emission.

4. process σ4 - direct band recombination and nonradiative recombination processes

Clearly, only processes σ1 and σ3a contribute to the creation of trapped electron so that the quantum efficiency of trapped electron creation S is

$$S = \frac{\sigma_1 + \sigma_{3a}}{\sigma_1 + \sigma_2 + \sigma_{3a} + \sigma_{3b} + \sigma_4} \tag{8}$$

According to the experimental data, S ≈ 10%. The fluorescence emission of processes σ2 and σ 3b are not useful, making it difficult to operate the device in the continuous mode. (It would be necessary to minimize the cross section of processes σ2, σ3b and σ4 for making the fluorescence emissions negligible compared with the IR stimulated emission.)

The arriving-electron trapping efficiency η_t for ET (in unit traps/J) is defined as

$$\eta_t = (1 - \eta_r) Y_l S \tag{9}$$

where η_r is the back scattering factor (the fraction of energy of back scatered electrons to primary electrons); Y_l is a limiting quantum yield for the pair creation (the inverse of average dissipated energy in creating one electron-hole pair). The trapping efficiency η_t is independent of the e-beam current density J until J reaches saturation, when all the traps are occupied and η_t starts to decrease. Since η_t is independent of the anode voltage V_a for some operating range of V_a, the total numbers of electron traps created per unit area during time period t is $n = JV_a t\eta_t$, based on which, the emission current density for saturating all electron traps in a ET film can be calculated. If the back scattering is $\eta_r \sim 0.15$, $Y_l \approx 1/2.1E_g$, S =0.1, and Eg = 4.3ev, then we have $\eta_t \approx 5.88(10^{16}$traps/J). In the saturation, all traps, i.e., all dopants of Eu^{2+} are occupied. The saturation current density is found as

$$J_s = \frac{ND}{V_a t \eta_t} \tag{10}$$

where N is the dopant concentration of Eu^{2+}, D is the penetrating distance of the energetic

electrons into the ET film, and t equals the frame time T divided by the number of pixels. If N = $10^{18}/cm^2$, anode voltage V_a = 1KV, t = 0.5 μs, and D = 1μm, then we have J_s = 3.4 A/cm^2. This current is close enough to a current for operating a emitter array. For example, one emitter tip can readily supply 10 μA and with a typical center to center spacing of 5 μm (4×10^6 tips/cm^2), the current density is 4 A/cm^2.

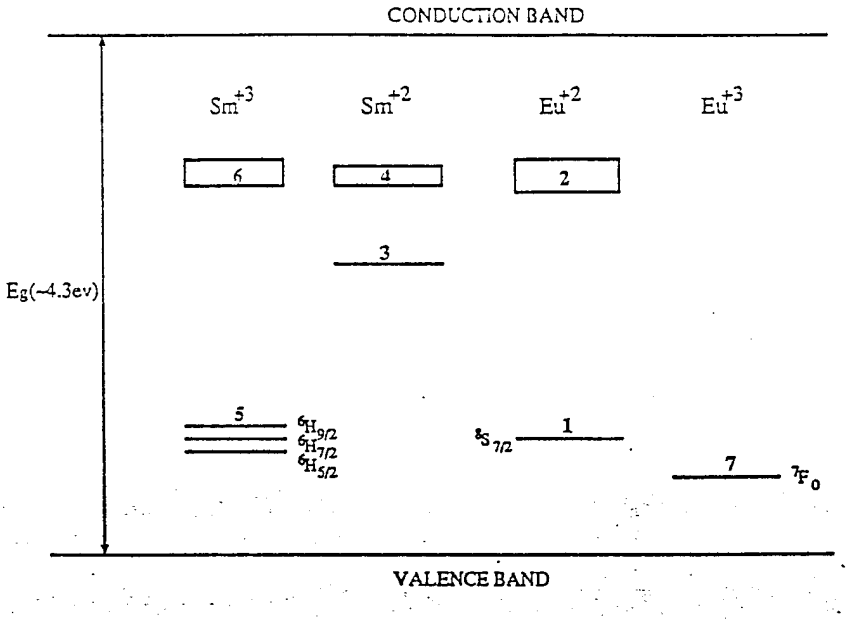

Fig. 3 Energy band diagram of ET materials

Since the Ce^{3+}/Sm^{3+} doped ET materials can be addressed by e-beam, it is then possible to combine a suitable ET phosphor layer with a matrix addressed field-emitter array to produce a novel versatile SLM with dual electron-optical and photo-optical addressability. The properties of the material which makes such a device attractive include its high sensitivity to ionizing radiation, wide dynamic range, and high spatial resolution. First, is has been shown that both SrS and CaS hosts are efficient ET phosphors for e-beam recording and retrieval. In both cases, a radiation exposure dynamic range of greater than 10^5 has been demonstrated, as shown in Figure 4. In addition, it is possible to achieve exceptional spatial resolutions with this approach. In the case of electron beam excitation of the material, the mean electron range within the material is about 1 μm when a 10 keV electron beam is employed. Thus, a phosphor layer of about 1 μm thickness would be sufficient to efficiently absorb electrons and maximize trapping efficiency.

A high resolution 1 μm ET phosphor layer can best be fabricated as a continuous thin film layer. Recently, we have developed the technique to fabricate polycrystalline ET thin films employing a multi-hearth electron beam vacuum deposition system. By suitably controlling the substrate temperature, the flux content supply, and deposition rate, polycrystalline ET thin films ranging from 1 μm to 40 μm have been fabricated. These ET thin films currently possess a

resolution of over 100 lp/mm and have the potential to reach 1,000 lp/mm if fabricated in monocrystalline forms. The response time of ET thin films to IR stimulation is measured to be on the order of ten nanoseconds. The linear dynamic range of the photoluminescent emission is about 40 dB.

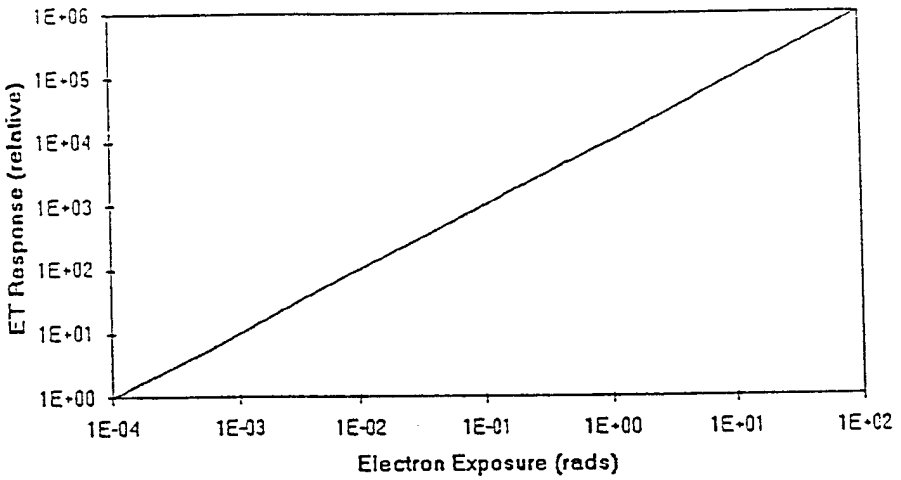

Fig. 4 A typical electron exposure response of ET materials

We have evaluated the performance of these polycrystalline ET thin films and investigated their compatibility with field-emitter arrays. A critical parameter is the electron trapping efficiency when stimulated by electron beam. A previous study has shown that the minimum energy to excite a trap is 5 eV and the quantum efficiency is about 10%.

The characterization of ET material under e-beam exitation was experimentally conducted. Quantex Q16 thin film samples were fabricated for their evaluations under both e-beam and IR excitations. The structure of the sample tested was as follows: 1mm thick sapphire substrate and four layers that were deposited on it. Four layers are: a 500 Å thick CaS-LiS layer for better adhesion and performance of the ET film, the second is a 4 μm Q16 film, above which are a 200 Å Al_2O_3 chemical barrier and a 200Å thick aluminum layer on the top. Before the deposition of the Al layer the sample was annealed at about 800 C°. The sample was evaluated with the modified scanning electron microscope (SEM) as shown in Fig. 5 , which shows the diagram of the geometry of the setup. Four LEDs that are 5 mm from the sample are utilized for IR stimulation. The intensity of IR radiated from four LEDs is about 20 mW/cm2 at a wavelength of 910 nm . An electron beam of prescribed current (electron flux) is generated by the SEM electrón

gun and projected onto the aluminized ET film biased at a given accelerating potential. After traps are excited in the ET film, the electron gun is turned off and the IR beam illuminates the ET film. The stimulated orange emission is detected as the measure of the trapped population. By changing the bias voltage and electron flux, the electron beam excitation efficiency can be characterized.

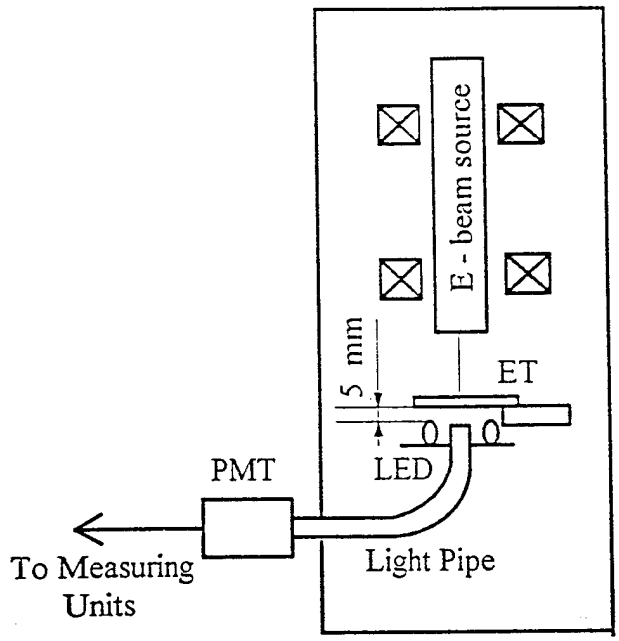

Fig. 5 Geometry of the setup for measuring the electron excitation efficiency of ET materials

A series of measurements were taken as the accelerating voltage was changed from 2 to 30 KV under a constant, 2 nA, e-beam current onto a target area of about 1 micron. The results are plotted in Fig. 6(a) and (b), in which the Y axis represents the output current of the detector (a PMT) in units of nA. The curve (peak IR response) was measured manually with 20 s (40 nC) excitation of the sample at the given voltage, and the IR was turned on after 5 seconds from the end of the exitation. This curve represents the initial peak value of the IR stimulated emission.

It can be seen on both curves of the diagram, that there is no significant response at range from 2 to 5 kV, but there is a threshold between 5 and 10 kV. (The SEM power supply happens to have no selectable intervening voltage.)

This provides information for determining the feasibility and design of a prototype of the proposed SLM. In this experiment, the minimum acceleration potential to produce writing to the ET film was also determined. The minimum anode potential is important because it determines the energy of electrons arriving at the aluminized surface of the ET thin film and hence the depth of

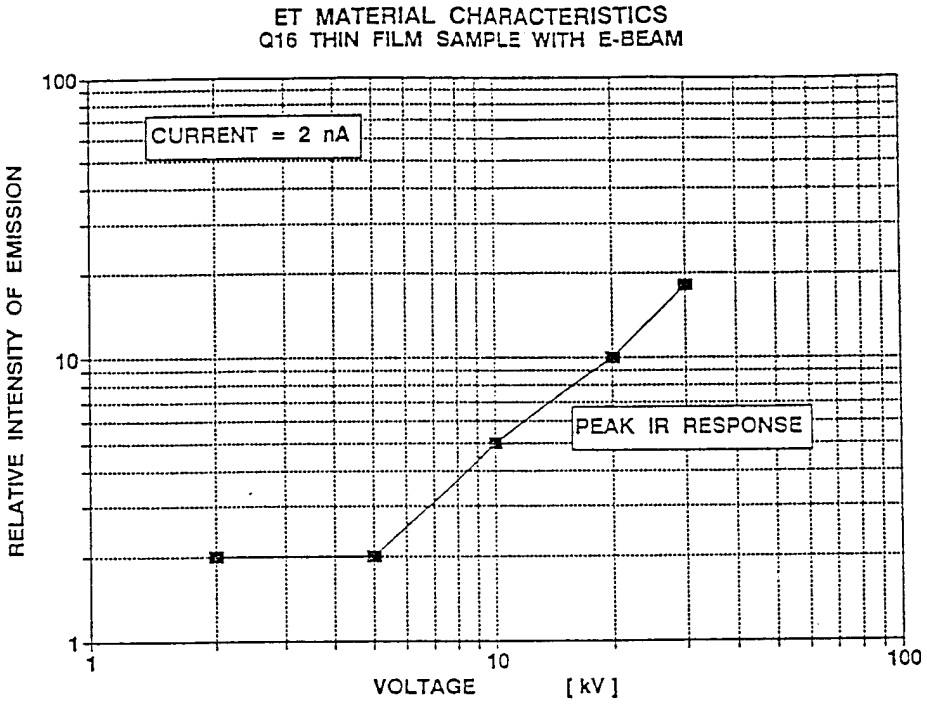

(a)

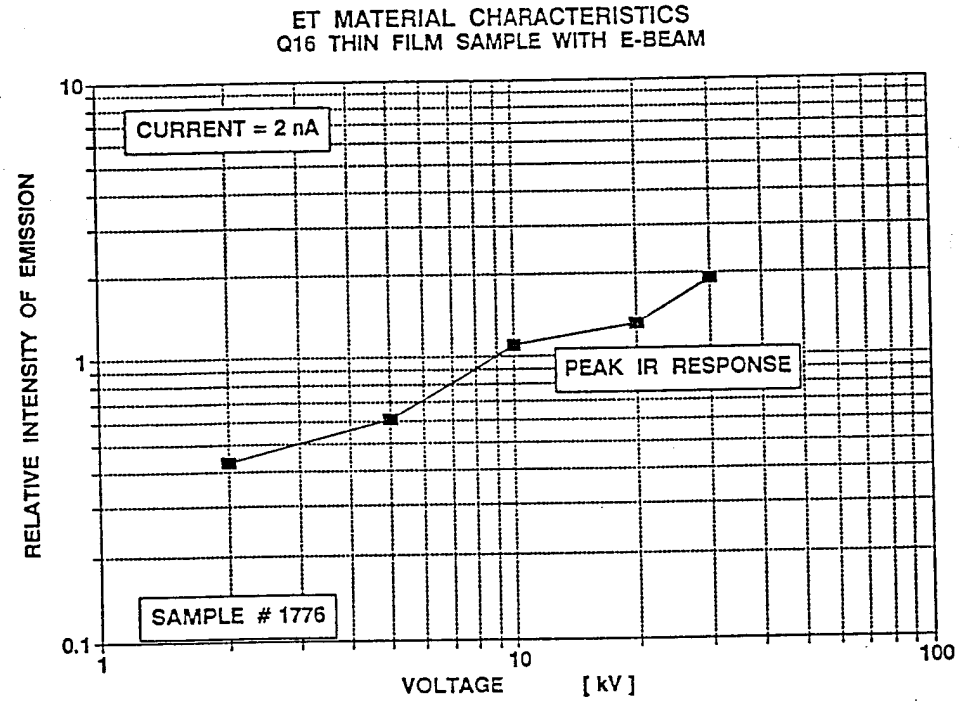

(b)

Fig. 6 The ET film characteritics of Q16 thin film under e-beam
(a) Q16 film with 200Å Al_2O_3 and 200Å Al coatings
(b) Q16 film with 200Å Al_2O_3 and 50Å Al coatings

penetration. The depth of penetration determines the number of available trappable electrons per pixel and, therefore, the current range and exposure time per pixel.

Another important parameter for the feasibility study is trap saturation density, i.e., the maximum number of traps within a given volume. It determines the dynamic range and the frame rate of the SLM. The maximum number of traps is related to the doping density of Eu and Sm in ET materials. Although we are confident to achieve a trap density of $10^{19}/cm^3$, the current Eu and Sm doping density has limited this number to about $10^{17}/cm^3$. In this Task, we have investigated the possibility to increase the saturation trap density by two orders of magnitude (to $10^{19}/cm^3$) by increasing the Eu and Sm doping density. As the doping density increases, it is very possible to face some continued segregation problems and difficulties. Effort will be made to overcome these difficulties by examining the feasibility of employing other means to implement the Ce and Sm.

2.3 Task 3 - Investigation of Device Architecture

The objective of this Task was to develop the architecture of the e-beam addressed SLM that incorporates the ET thin film with a field emitter array. A basic configuration is illustrated in Fig. 7 (a) and (b). A layer of ET film is deposited on a ITO-coated fibre-optic faceplate. The ITO transparent electrode, biased at about 1KV, serves the role of both acting as the field emission anode and preventing charge accumulation on the ETM surface due to both primary and secondary emission electrons, The ET film and a matrix-addressable field-emitter array are cascaded and sealed in a vacuum assembly. The distance between the ET film and field-emitters is determined by the height of the space pillar. Usually this distance is very small to allow proximity coupling of gated emitter tips and the ET thin film. The crossings of the X-Y matrix addressing electrodes represent individual pixels which contain many micro field emitters. The inclusion of many field emitters in each pixel is to average out the emission fluctuation and noise of single emitter.

The operation of the SLM is described as follows: An electrical signal addresses the field-emitter array through the orthogonal gate and base electrodes. The current generated from each emitter tip is proportional to the control voltage between the electrodes. These electrons are accelerated by the high bias voltage and are projected onto the ET thin film. Electron traps are excited in the ET film at the areas that are exposed to the writing electron beams. An IR light then illuminates the ET film from the back side. It releases the trapped electrons from the trap sites and stimulates orange emission. The intensity of orange emission is proportional to the product of the intensity of electron writing beam (hence the input electrical signal) and the intensity of the IR reading beam. The device works as a typical electrically-addressed reflective incoherent SLM. In the second operation mode, the proposed SLM can be addressed simultaneously by an electrical input and an optical input. The output is the emitted orange light from ETM, carring the pattern embodied in the addressing e-beam.

As we discussed in previous sections, field-emitter arrays can also be addressed by visible light [21] (see Fig. 7(a), light illuminating the device from bottom). Therefore, the proposed SLM can also work in an optically-addressed mode. Furthermore, the IR light illuminating the ET film can also carry a 2-D spatial signal (e.g., imagery) which behaves as the third input. The output is the interaction between the electrical and optical inputs. This is the unique feature that no other state-of-the-art SLM possesses at this time. Since the ET film and the field-emitter array may work separately, all the inherent operational modes of the ET based SLRs and SLMs, such as optically addressed operation, incoherent-to-coherent conversion (with a narrow band-pass filter added), coherent modulation, and storage mode are preserved in the proposed SLM.

The X-Y matrix addressing machnism has been considered that the driver circuit must have a built-in option for two modes of operations, that is one frame mode and one continuos mode, as discussed above. It has been shown recently that for cesiated emitters, the field emission requires a threshold voltage of only ~15V with a swing range of ~10V [5]. Such a low voltage of operation make it possble to build the driver circuit based on VLSI technology with computer interface. Figure 8 shows one possible timing scheme for the driver circuit. The Y electrodes (connected to emitter tips) select sequentially one column of pixels at a time for addressing, that is, V_Y =-15V for selecting and V_Y= 15V for unselecting. The X electrodes (connected to the gates) carry the data (0 < Vx < 10V) for each column of pixels. The frame time T could be greatly varied. The upper limit of T is dictated by the requirement of $\beta I_{IR} T \ll 1$ for continuous operation with simultaneous IR illumination. This requirement should be satisfied for typical operating conditions as long as T < 100ms. The low limit of T should satisfy the requirement in the frame mode of operation, the field emission current should be able to create filled electron traps that cover the whole available wide dynamic range (>40dB). This requirement is determined by the maximum available field emission current and the level of traps in the ET media (dopant level and thickness of the film). The low limit of T will be most likely limited by the large capacitances existing between the thin film electrodes (gates and emitters) and the substrate.

The field emitter array can be fabricated to have pixels with center to center spacing of 3.2 μm [28] and the polycrystalline ET film has demonstrated a resolution limit of 100 lp/mm. The resolution of the proposed SLM device is limited by the transverse dispersion of the e-beams, which emerge from the emitters and travel towards the ET panel under the acceleration of the anode voltage. The transverse dispersion distance δ is given by [28]

$$\delta = 2d \sin \vartheta \frac{(V_G)^{1/2}}{(V_A - V_G)} [(V_A - V_G \sin^2 \vartheta)^{1/2} - (V_G)^{1/2} \cos \vartheta] \qquad (11)$$

where d is the distance between the gate film and the ET panel; θ is the angle between the emerging electrons and the normal direction; V_A and V_G are the anode and gate voltage, respectively. The equation shows that d should be minimized to achieve a maximum resolution.

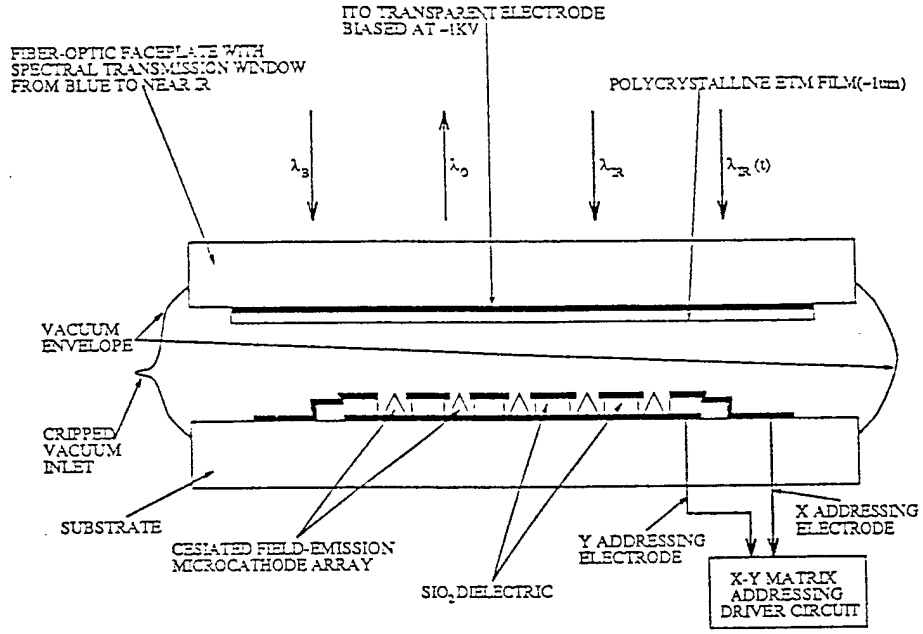

(a)

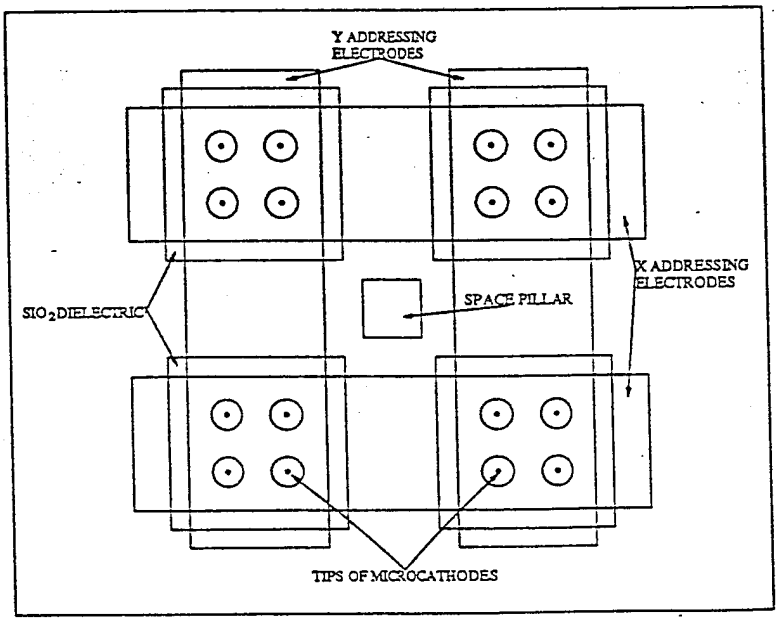

(b)

Fig. 7 E-beam adressed emissive spatial light modulator
(a) front view of the SLM, (b) top view showing the pixel structure

For V_A = 1000V and d =100 μm, the electric field between the gate film and the ET panel is about 1X10^5 V/cm, which is approaching the practical vacuum ionization/breakdown limits. Assuming d = 100μm and a maximum angle θ = 30°, Figure 9 shows the dispersion distance δ as a function of the gate voltages for anode voltage of 500V, 1000V, and 1500 V, respectively. For V_A = 1000V and V_G < 30V, δ is less than 15 μm. In order to avoid crosstalk, emission electrons from one pixel should not arrive at an adjacent pixel on the ET panel,. Thus δ should be less than the seperation between pixels. If the pixel size is equal to the pixel seperation (15 μm) the resolution limit is 33 lp/mm. Since both ET film and the field emitter array could be fabricated on large substrates, the potential space bandwidth products of the proposed SLM is extremely high. For example, for having 2000X2000 pixels, the whole array is 3" by 3".

The anode voltage *Va* must satisfy a few conditions to operate the proposed SLM. First, higher resolution requires small distance from gates to anode and high anode voltage, as discussed early. But there is a maximum voltage that causes vacuum breakdown. Second, further research must be performed both theoretically and experimentally to determine the anode voltage as a function of both the electron trapping efficiency η_t and penetrating distance D. The electron trapping efficiency dependence on anode voltage η_t (*Va*) behaves similarly to that of CRT

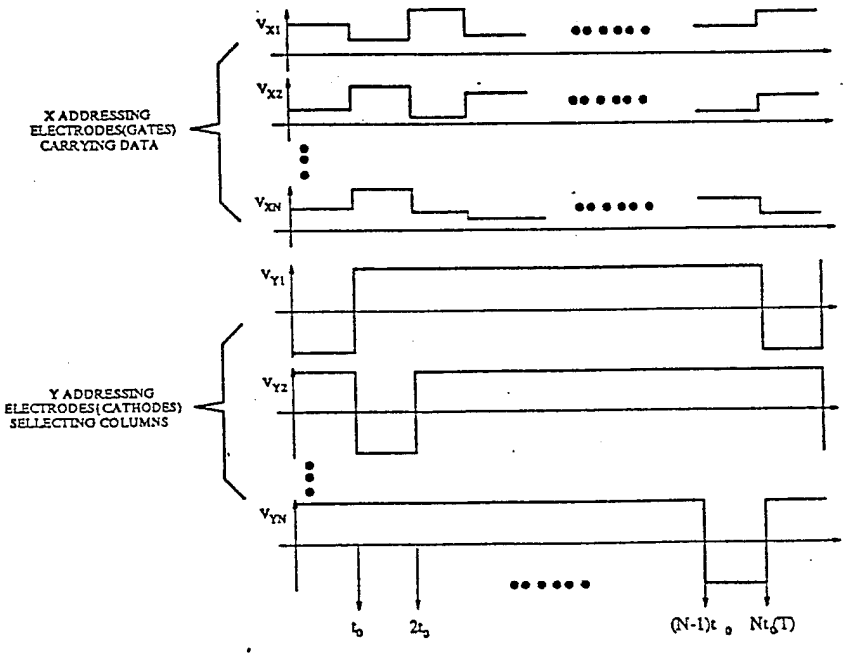

Fig. 8 Timing diagram of the X-Y matrix driver circuit

phosphors. Figure 10 shows a typical curve of such a dependence. The voltage V_o is the so-called dead voltage which (also region (1)) is due to nonradiative recombination processes in the layers overlying the surface of ET film and must be overcome for proper operation. Region (2) is the usual range of operating voltage, in which the trapping efficiency is constant, and region (3) corresponds to the saturation where electrons have completely penetrated the ET film. The dead voltage *Va* of ET film has to be determined in order to select an operating anode voltage that lies in region (2). The penetrating distance dependence on the anode voltage can also be determined. There would likely be a tradeoff between the dynamic range and resolution of the SLM based on the selection of the anode voltage. A wider dynamic range would require the electrons penetrate more deeply into the ET film, thereby requiring higher anode voltage. This, however, may require a larger distance of the gate to anode to prevent the vacuum breakdown, resulting in low resolution. Optimum overall performance of the SLM would be obtained for a specific anode voltage.

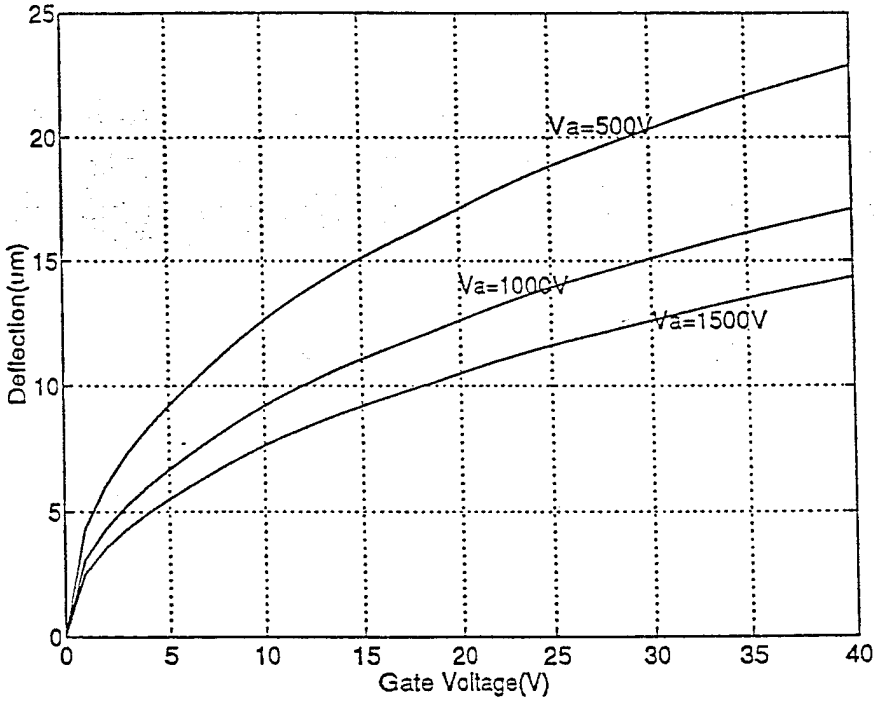

Fig. 9 Dispersion distance as a function of gate voltage

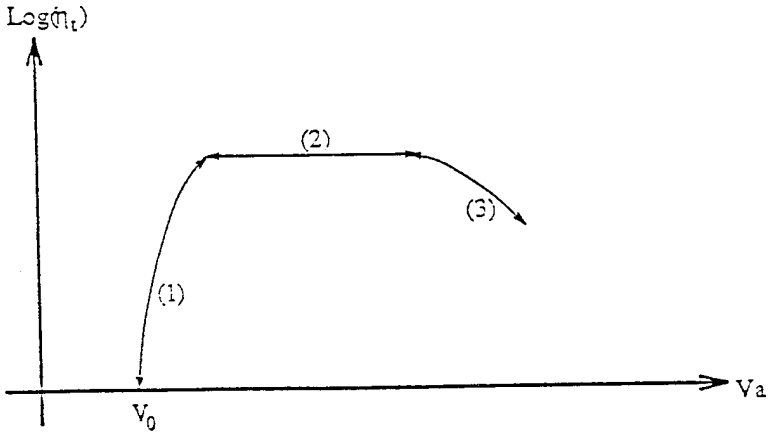

Fig. 10 Variation of electron trapping efficiency with anode voltage

2.4 Task 4 - Engineering Design of a Prototype Device

To further evaluate the technical and manufactural feasibility and the potential performance of the proposed e-beam addressed SLM, a 128X128 pixel prototype device is planned to be fabricated and tested in the next development phase. Schematic diagrams of the prototype are shown in Fig. 7(a) and Fig 7(b).

A field emitter array provided by SRI International will be uesd for the fabrication of the proposed SLM. Each pixel of the SLM composes od 10 x 10 field emitter tips os that the whole SLM array contains 1280X1280 emitter tips. The center-to-center distance of emitter tips is designed to be 5 μm, which is compatible to the SRI's fabrication capability and may be subject to change due to the device availability. If the center-tocenter distance is 5 μm, each pixel of the SLM measures 50 X 50 μm^2 and the whole active area of the SLM measures only 6.4 X 6.4 mm^2, which is in the same order of (or smaller than) most of the state-of-the-art SLMs.

An ET thin film coated with AL_2O_3 and aluminum Al is placed on the top of the field emitter array, as shown in Fig.7(a). The substrate is 0.5 mm thick sapphire, whose surface flatness is required to be λ/4 at least and the thickness error is less than 1 μm. The thickness of the ET layer is between 1 to 3 μm, the AL_2O_3 layer is coated to a thickness of 50 Å , and the aluminum coating is 50Å . Four space pillars are located at each corner to keep a distance between the ET

film and the surface of the emitter array as required to be 25 μm, which is a compromise between the bias voltage and the resolution.

The address electrodes are built-in in the field emitter array. The X-Y addressing scheme is the same as discussed in the previous sections. Although a low control voltage (10 - 15 V) is possible for operation with the cesiated device, the SRI device will be used for the prototype development because of its reliability. The controlvoltage is 30 - 50 V. This is still viable with present available electronic components.

If the current is 0.5 μA per tip, the maximum current (when all pixels are turned on) is only 0.8 A and the power consumption by the SLM is only about 30W.

The device will be packaged at Thomas Electronics Inc's facilities. The ET panel and the field emitter array is sealed in a vacuum package with electronic leads connected outside. The pressure within the package is required to be lower than 10^{-9} Torr.

It should be noted that this is only a preliminary design (or specification determination). A detailed design will be done during the early stage of the Phase II program.

2.5 Task 5 - Investigation of Various Applications of the Proposed Device

The proposed e-beam addressed SLM is primarily an incoherent SLM but has also the capability of performing coherent modulation. It combines large SBP, high frame rate and high contrast ratio in a single device. It also has a wide variety of operational modes and, more importantly, the electrical and optical dual-addressability. The proposed SLM offers more versatility and application flexibility than all the state-of-the-art SLMs. By taking advantage of these unique features, performance of the current optical processing systems can be substantially improved and novel architectures that are not implementable with other SLMs can be developed. Special attention will be given to optical processing systems that benefit from unique features of the proposed device such as its extremely wide dynamic range. An example is learning in photonic neurocomputing where wide dynamic range and fast weight update are needed. Other areas that could benefit from the wide dynamic range are optical wavelet transform and a transform camera concept that can produce, for example, the Fourier transform of a natural scene via the projection-slice theorem without resort to incoherent-to-coherent image conversion [22]. Both systems require wide dynamic range "kernel" masks in their operation. Other applications that are related to NASA's missions and would benefit from the merits of the proposed devices will also be explored.

It has been reported [30] that an optoelectronic pulsating neuron can be generated by combining the dynamic property of ET with theS-shaped nonlinear I-V characteritic of a programmable unijuction transistor. When ETs are exposed to a static blue light , astatic IR light, and a pulsed IR light, they are suited for implementing dense synatic weights with nondestructive readout in optical neural networks of pulsating neurons [26]. It is possible to build a dense array of photonic pulsating neurons by combining the dynamic of ET's with S-shaped I-V chracteristic of unijuction transistors.

Under simultaneous blue light and IR light ilumination, the dynamic of ET is obtained as (similar to Eq. (1) and (2))

$$\frac{dn(t)}{dt} = \alpha I_B(t) - \beta n(t) I_{IR}(t), \tag{12}$$

$$I_O(t) = \kappa I_B(t) + \gamma n(t) I_{IR}(t), \tag{13}$$

where $I_B(t)$, $I_{IR}(t)$, and $I_O(t)$ represent the blue light, IR light, and the emitted orange light intensities, respectively; For simplicity, the coefficients α, κ, β, and γ can be assumed as constants to a first order approximation. If $I_{IR}(t)$ is static and $I_B(t)$ consists of astatic term and a pulse modulated term, as follows:

$$I_B(t) = I_0 + I_1 \sum [u(t - kT) - u(t - kT - t_w)] \tag{14}$$

where u(t) is step function, I_0 and I_1 are the static and pulse blue light intensities; and T and t_w are the pulse period and pulse width. Thus the emitted orange light is given by :

$$I_O = \begin{cases} \kappa(I_0 + I_1) + \dfrac{\alpha\gamma I_0}{\beta} + \alpha\gamma I_{IR}\left\{\dfrac{t_w}{\exp(\beta I_{IR} T) - 1} + t - NT\right\} \\ \kappa I_0 + \dfrac{\alpha\gamma I_0}{\beta} + \alpha\gamma I_1 I_{IR} t_w \dfrac{\exp[-\beta I_{IR}(t - NT - t_w)]}{1 - \exp(-\beta I_{IR} T)} \end{cases} \tag{15}$$

where N >>1, and $\beta I_{Ir} t_w << 1$. It can be seen that the IR stimulated emission and the fluorescence effect are mixed together in the emitted orange light. Fluorescence is manifested by sudden jumps at the onset and termination of the blue light pulse. Ir stimulated emission, on the other hand, undergoes a linear increase first and then decays exponentially after the pulse in the discharging process.

An experiment has been performed to verify the above dynamic process with the setup shown in Fig. 11. One beam from an Argon laser provides the static blue light by passing through a pair of polarizers that allow the value of I_0 to be adjusted. Another beam provides the pulse light by passing through the progammble liquid crystal gate. The IR collimated light comes from a fibre coupled diode laser. The orange light emission from the ET panel is filtered by an orange filter and detected by a photomultiplier, whose photocurrent is coverted into voltage and displayed on a digital oscilloscope. Figure 12 shows a typical oscilloscope curve of the ET

response when I_0=0.2 mW/cm2, I_1 = 14.4mW/cm2, I_{IR} = 418 mW/cm2, t_w = 10ms, and T = 80ms. One observes that the fluorescence jumps at the blue light pulse edges, linear buildup during the pulse, and exponential decay after the pulse, as predicted by above equation.

The setup in Fig.11 is incorporated with a PUT circuit so as to form an optoelectronic pulsating neuron. The electronic portion of the system is shown in Fig. 13, along with the I-V characteristic of PUT. As shown in Fig. 13, the photocurrent from the photomultiplier is converted into voltage, drving the grid of the PUT. The cathode voltage of the PUT is fed back and remotely controls the liquid crystal gate. Suppose now that the orange light undergoes a jump such that the grid voltage of PUT, V_G, is above the threshold ,V_{th}, and the PUT is cut off. When the downward relaxation of V_G reaches V_{th} from above, the PUT sudenly conducts and goes into cutoff quickly, following the limit-cycle trajectory shown in Fig. 13. The conducting of the PUT briefly opens the liquid crystal gate, thus producing a blue light pulse, which can be regarded as the optical spike or action potential of the system. The blue light pulse illuminating the ETM produces another jump in the emitted orange light I_o, and the system enters self-sustained oscillation. The interspike interval T is determined by how fast the orange light relaxes so that V_G rechches V_{th}. The orange light relaxation can be controlled by both the static blue light I_0 and the static IR light I_{IR}. I_0 and I_{IR} play roles analogous to excitatory and inhibitory neurotransmitters in biological neurons.

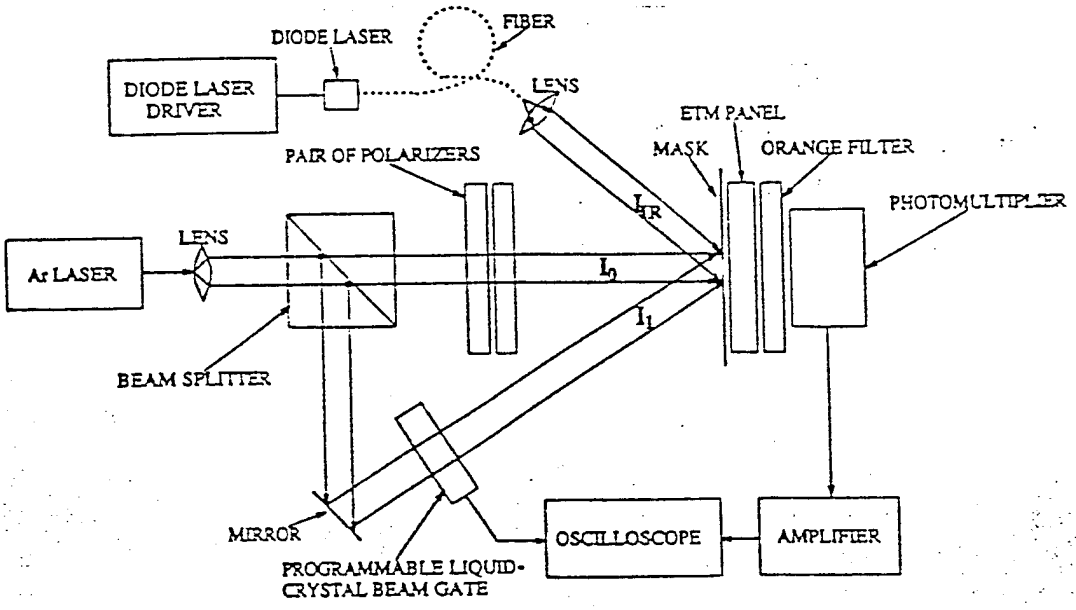

Fig. 11 Experimental setup for studying the dynamics of the process

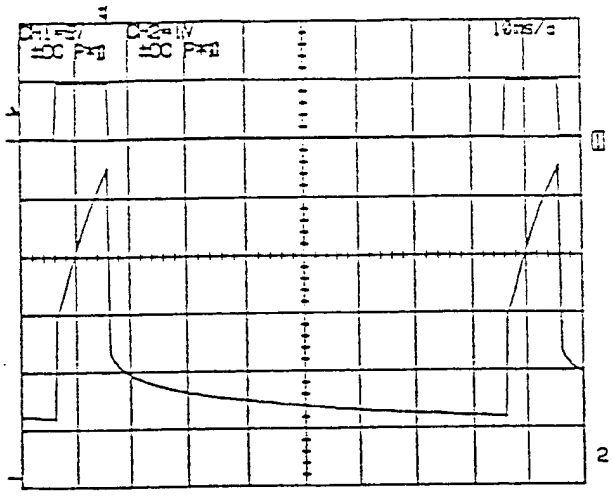

Fig. 12 Oscilloscope display of the ET response: upper trace is pulsing signal from the programmable beam gate; lower rtrace, ET response.

Figure 14 (a) and (b) show the oscilloscope display of the experimental results for different values of I_0 and I_{IR}. As can be seen, by varying the the static blue light intensity I_0 one has the ability to control the interspike interval T. The same is true with varying IR light intensity I_{IR}. It is worth noting that if I_0 is high enough that V_G never reaches V_{th} the firing is suppressed altogether, i.e., T $\rightarrow \infty$. One expects that when I_0 and I_{IR} contain superimposed periodic modulations, the system would exhibit complex phase-locked firing dynamics [31,32]. Recent physiological experimental results strongly suggest that temporal information, such as correlation and coherence in the firing activity of neurons, plays a role in higher-level brain functions such as feature-binding and cognition [33,34].

The optoelectronic pulsating neuron combining the ET and the PUT has the potential of producing dense arrays of optically coupled pulsating neurons of the order of $10^3 - 10^4$ elements, when eventually ET's would be used with a smart-pixel SLM based on integrated optoelectronic cellular array technology[35], or liquid-crystal-on-silicon VLSI technology[36]. Building such dense array ofpulsating neurons would be an important first step toward building a new generation of neural networks that use synchronicity, bifurcation, and chaos in producing higher-level cortical functions.

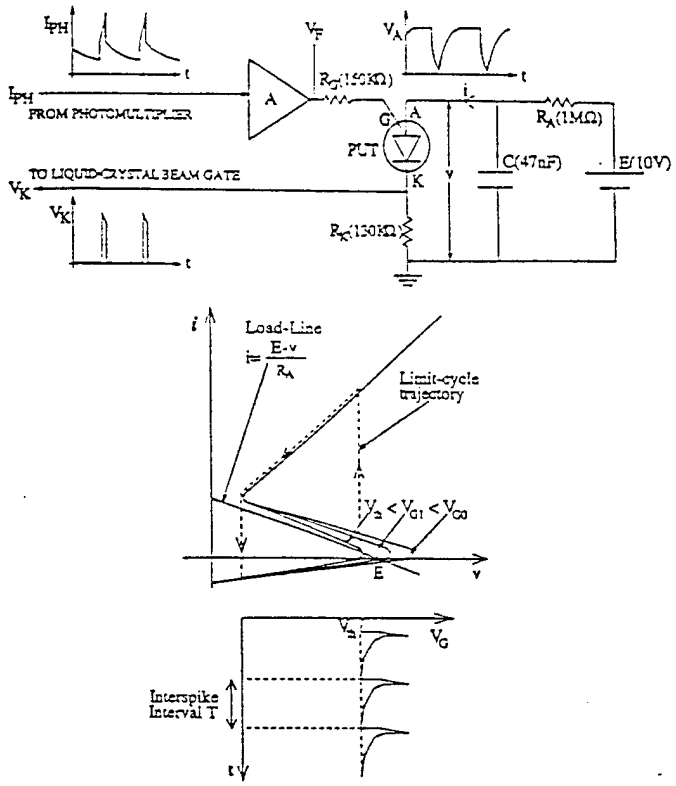

Fig. 13 PUT circuit used in the optoelectronic pulsating neuron experiment and the I-V characteritic of the PUT

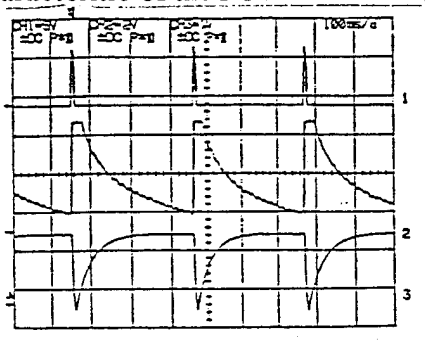

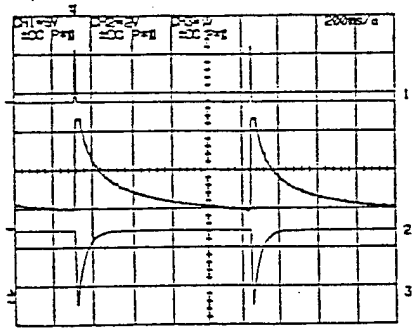

Fig.14 Oscilloscope display of the optoelectronic pulsating neuron:
Upper trace, cathode voltage of PUT ,V_K representing the pulsating blue light.
Middle trace, representing the orange light relaxation.
Lower trace, anode voltage of the PUT,

3. CONCLUSIONS

A novel e-beam addressed SLM was proposed and investigated. It combines the patented polycrystalline ET materials with the state-of-the-art electric field emitter array to achieve high resolution, high SBP, high update speed and high contrast ratio. The objective of the Phase I work was to determine the technical feasibility of the proposed SLM.

This objective has been successfully achieved. During the Phase I period, we reviewed the current development status of the field emitter array and established collaboration or contact with a few companies working in this area. The performance of ET thin film under e-beam excitation has been investigated intensively. Based on the promising results obtained from these investigations, we have finalized the configuration and addressing scheme of the e-beam addressed SLM. A128 X 128 pixel prototype device was designed and was planned to be developed in Phase II.

4. RECOMMENDATIONS FOR PHASE II

The following tasks are suggested for the Phase II program:

1. Fabrication and delivery of the field emitter array

   Field emitter array is one of the two key components in the prototype device to be developed in Phase II. At the first stage of the project, a few field emitter arrays should be fabricated by a subcontractor, e.g., SRI International Inc., and delivered to Quantex. These field emitter arrays should have 12,800 x 12,800 emitter tips and with built-in matrix addressing electrodes.

2. Development of high performance ET thin film

   The Phase I results showed there is still a margin in the performance of ET thin film under e-beam excitation. In Phase II, An effort should be made to further improve the performance of ET films. High quality ET thin film is deposited on sapphire substrates and then coated with the anode layers. The thickness of the ET film and the anode layers as well as their quality will be optimized through simulation, experiment and fabrication.

3. Evaluation of V_a, resolution, writing response and outgassing

   The trade-offs between these parameters would be evaluated to determine the design parameters for the prototype dually addressed SLM.

4. Assembly of the protoytpe of e-beam addressed SLM

The emitter array (with addressing electronic leads) and the ET thin film structure would be assembled into a vacuum package. The required pressure in the package is likely to be about 10^{-9} Torr. This could be done either at Quantex or by a subcontractor (e.g., Thomas Electronics Inc.).

5. Driver circuit design and fabrication

The X-Y matrix addressing driver circuit (as discussed in section 2.3 in this report) would be developed. For the field emitter array uesd in the prototype development, the threshold voltage is 30 V and the swing range is about 15 V the driver circuit would be designed and fabricated in the form of a circuit board capable of interfacing with the computer. It should also be compatible with analog video signals obtained from CCD cameras and digital video signals generated by frame grabbers.

6. Characterization and evaluation of the prototype

The prototype device would be experimentally evaluated and its specifications would be measured. The performance potential and limitations would be studied. Suggestions on the structure and specifications to improve its performance and commercial manufacturability would be provided.

7. Application development

Various applications of the e-beam addressd SLM that take advantage of its unique properties would be studied. New concepts and architectures could be expected from such studies.

5. REFERENCES:

[1]. J.A.Davis, J.Gamlilie and G.W.Bach, "Optical transmission and contrast ratio studies of the magnetooptic spatial light modulator," Appl. Opt., 27, 5194(1989).

[2]. D.R.Pape, "Multichannel Bragg cells: design, performance and applications," Opt. Eng., 31, 2148(1992).

[3]. K.Sayyah, U.Effron, C.S.Wu and S.T.Wu, "Single crystal silicon LCLV with one millisecond response time," pp.189-194 in Tech. Digest on SLM and Applications, (OSA, Washington, DC, 1990).

[4]. H.K.Liu and T.H.Chao, "Liquid crystal television spatial light modulator," Appl. Opt., 28, 4772(1989).

[5]. K.M.Johnson, D.A.Jared, T.Slagle, K.Wagner, C.Mao and M.G.Robinson, "Ferro-electric LC-SLMs and applications," pp.90-93 in Tech. Digest on SLM and Applications, (OSA, Washington, DC, 1990).

[6]. D.A.Gregory, R.D.Juday, J.Sampsell, R.Gale, R.W.Cohn and S.E.Monroe, :Optical characteristics of a deformable mirror SLM," Opt., Lett., 13, 10(1980).
[7]. C.Warde and J.I.Thackara, "Operating mode of the microchannel spatial light modulator," Opt. Eng., Vol. 22, 695(1983).
[8]. L.M.F.Chirovsky, L.A.D'Asaro, C.W.Tu, A.L.Lentine, G.D.Boyd and D.A.B.Miller, "Batch-fabricated self electro-optic effect devices," pp.2-6 in OSA Proc. Photonic Switching, (OSA, Washington DC, 1989).
[9]. C.Warde and A.D.Fisher, "Spatial light modulators: applications and function capabilities," pp477-523 in Optical Signal Processing, J.L.Horner ed., (Academic Press, San Diego, 1987).
[10]. J.A.Neff, R.A.Athale and S.H.Lee, "Two-dimensional spatial light modulators: a tutorial," Proc. IEEE, 78, 826(1990).
[11]. J.Lindmayer, "Photoluminescent materials for optical upconversion," US Patent 4,839,092(1989).
[12]. S.Jutamulia, G.M.Storti, J.Lindmayer and W.Seiderman, "Use of electron trapping materials in optical signal processing. 1: parallel Boolean logic," Appl. Opt., 29, 4806(1990).
[13]. S.Jutamulia, G.M.Storti, J.Lindmayer and W.Seiderman, "Use of electron trapping materials in optical signal processing. 2: 2-D associative memory," Appl. Opt., 30, 2879(1991).
[14]. A.D.McAulay, J.Wang and C.Ma, "Optical heteroassociative memory using spatial light rebroadcastors," Appl. Opt., 29, 2067(1990).
[15]. X.Yang, W.Seiderman, R.A.Athale, M.Astor and N.P.Caviris, "Optical implementation of winner-take-all neural network using electron trapping materials," Opt. Commun., 93, 33(1992).
[16]. X.Yang, C.Wrigley, J.Lindmayer and D.A.Gregory, "Compact joint transform correlator using electron trapping spatial light modulator," Optik, 93, 35(1993).
[17]. X.Yang, C.Wrigley and J.Lindmayer, "Three-demensional optical memory based on transparent electron trapping thin films," Proc. SPIE, 1773, (1992).
[18]. C.A.Spindt, C.E.Holland, I.Brodie, J.B.Mooney and E.R.Westerberg, "Field-emitter arrays applied to vacuum fluorescent display," IEEE Trans. Elec. Dev., 36, 225(1989).
[19]. C.A.Spindt, C.E.Holland and I.Brodie, "Field-emitter arrays applied for vacuum microelectronics," IEEE Trans. Elec. Dev., 38, 2355(1991).
[20]. J.M.Macaulay, I.Brodie, C.A.Spindt and C.E.Holland, "Cesiated thin-film field emission microcathode arrays," Appl. Phys. Lett., 61, 997(1992).
[21]. R.N.Thomas, R.A.Wickstorm, D.K.Schroder and H.C.Nathanson, "Fabrication and some applications of large-area silicon field emission arrays," Solid-State Elec., 17, 155(1974).
[22]. P.R. Schwoebel, and C.A. Spindt, "Glow discharge processing to enhance field-emitter array performance," J. Vac. Sci. Technol. B 12(4). Jul/Aug. (1994)
[23] C.A. Spindt, C.E. Holland, A. Rosengreen, and I. Brodle, "Field-emitter-array develpment for high frequency operation," J. Vac. Sci. Technol. B 11(2), 468-473, Mar/Apr. (1993)
[24] C.A. Spindt, C.E. Holland, I. Brodle, P. Schwoebel, R. Kubena, and F.Stratton, "The fabrication and performance of gated field-emitter-array with nanometer feature sizes," Seventh International Vacuum Microelectronics Conference. Grennoble, France, July 4-7

(1994)
[25] P.R. Schwoebel, and C.A. Spindt, and I. Brodle "Electron emission enhancement by overcoating field-emitter array with titanium, zirconium, and hafnulm," Accepted for publication in J. Vac. Sci. Technol. B (1995)
[26]. Z.Wen, N.H.Farhat and Z.J.Zhao, "Study of the dynamics of electron trapping materials for use in optoelectronic neurocomputing," Appl. Opt., 32, 7251(1993).
[27] J. Keller, J. Mapes, and G. Cheroff, "Studies on some infrered stimulable phosphors," Phys. Rev. 108, 663-676 (1957)
[28] I. Brodle, and C.A. Spindt, "Vacuum Microelectronics," in Advances in Electronics and Electron Physics, Vil. 83, Academic Press, 1992, pp 1-106
[29]. N.H.Farhat, C.Y.Ho and S. Y. Lin, and L. S. Chang, "Projection treorems and their applications in multidimensional signal processing," Proc. SPIE, 388, 19(1983).
[30] Z.Wen, N.H.Farhat and S. Y. Lin, "Pulsating neuron produced by electron-trapping materials," Optics Letters 19, 1395 (1994).
[31] N. H. Farhat and M. Elderfrawy, Proc. Soc. Photo-Opt. Instrum. Eng. 1773, 23 (1992)
[32] N. H. Farhat, S. Y. Lin, and M. Elderfrawy, Proc. Soc. Photo-Opt. Instrum. Eng. CR55,77 (1994)
[33] C. M. Gray and W. Singer, Proc. Natl. Acad. Sci. (USA) 86,1698 (1989)
[34] R. Eckhorn, H. J. Reitboeck, M. Arndt, and P. Diche, Neural Comput. 2, 293 (1990)
[35] M. K. Hibbs-Brenner, S. D. Mukherjee, J. Skogen, B. Grung, E. Kalweit, and M. P. Bendett, Proc. Soc. Photo-Opt. Instrum. Eng. 1563, 10 (1991)
[36] K. M. Johnson, D. J. McKnight, and I. Under wood, IEEE J. Quantum Electron. 29, 699 (1993)